ISSN 8755-6839

SCIENCE OF TSUNAMI HAZARDS

Journal of Tsunami Society International

Volume 40 Number 1 2021

SIMULATION OF TSUNAMI ALONG NORTH SUMATRA AND PENINSULAR MALAYSIA ALLIED WITH THE INDONESIAN TSUNAMI OF 2004 USING A SHALLOW WATER MODEL

Md. Fazlul Karim

Department of Mathematical and Physical Sciences, East West University, Dhaka-1212, Bangladesh

Email: fkarim@ewubd.edu

ABSTRACT

The linear polar coordinate shallow water model of Ismail et al. (2006) is used to simulate Tsunami effect along North Sumatra and Penang Islands allied with Indonesian tsunami of 2004. The study of Ismail et al (2006) was based on the assumption that the primary displacement of the water surface at the source zone in the form of sea level rise and fall is equal to the stationary move of the sea floor deformation in the rupture region, which is not completely precise. The dynamics of seafloor displacement over a short period of time was ignored in that study. The major factor, which determines the initial amount of a tsunami, is the amount of vertical sea floor deformation (Iguchi, 2011). The properties of Indonesian tsunami 2004 are related to the scale of the bottom displacement (Kowalik et al. 2005). In this paper, a reassessment of the initial tsunami source of 2004 Indonesian tsunami taking the amount of vertical sea floor deformation and the dynamics of seafloor displacement over a short period is considered as the initial condition of tsunami generation. The computed maximum water levels along the coastal belts of Sumatra and Penang in Peninsular Malaysia compare well with the observed water level data obtained through post tsunami surveys. The results of this study suggest that a linear cylindrical polar coordinate shallow water model can be applied to simulate different aspects of tsunami.

Keywords: *Indonesian Tsunami 2004, Shallow Water Equation, North Sumatra, Peninsular Malaysia*

1. INTRODUCTION

On December 26, 2004 a shocking mega thrust earthquake happened along 1200 km of the subduction zone west of Sumatra and Thailand in the Indian Ocean with an intensity of Mw = 9.0 having Epicenter at 3.32° N, 95.85° E (Yalciner et al. 2005). The earthquake also activated a massive tsunami that propagated throughout the Indian Ocean and caused extreme inundation and extensive damage along the coasts of 12 rim countries of the Indian Ocean.

With the present level of knowledge it is feasible to simulate tsunami propagation by (Imamura et al. 1996, Titov and Gonzalez 1997, Imteaz and Imamura 2001, Kowalik et al. 2005, Roy and Izani 2005). The numerical approaches allow complete flexibility in specifying tsunami source regions and generation mechanisms.

A cylindrical polar coordinate model ensures very well resolution near the coast and coarse resolution away from the coast by suitably locating the Pole near the coast (Roy et al 1999). Haque et al.(2003) improved the model of Roy et al. (1999) for achieving finer resolution along the coastal belt of Bangladesh. Using the concepts of these two studies Ismail et al (2006) developed a shallow water model in Cylindrical Polar coordinates to simulate the tsunami along the coastal belts of North Sumatra and Penang Islands allied with 2004 Indonesian tsunami.

Karim et al (2016) simulated propagation of 2004 global tsunami generated by the sea bed deformation using a non-linear polar coordinate shallow water model. Roy et al (2007) developed a non-linear polar coordinate shallow water model for tsunami computation along North Sumatra and Penang Island in peninsular Malaysia. Karim et al. (2007) developed a shallow water model for computing Tsunami along the west coast of Peninsular Malaysia and Thailand using boundary-fitted curvilinear grids.

In this study, the linear polar coordinate shallow water model of Ismail et al. (2006) has been used to simulate the effect of 2004 Sumatra tsunami taking into account the initial sea floor deformation as an initial condition of tsunami source generation. This model is extending from Penang in Peninsular Malaysia to the west of Sumatra Island in Indonesia and the source of the Indonesian tsunami is within the model domain. The model has also been applied to simulate other related features of tsunami surrounding these Islands.

2. MATHEMATICAL FORMULATION

2.1. *Governing Equations*

A Cylindrical Polar coordinate system is defined where the Pole, O, is at the undisturbed level of the sea surface ($r\theta$-plane) and Oz is directed vertically upwards. The displaced position of the free surface is $z = \zeta\,(r, \theta, t\,)$ and the position of the sea floor is $z = -\,h\,(r, \theta\,)$, so that the total depth of the fluid layer is $\zeta + h$. Following Roy et al. (1999), the depth-averaged linear shallow water equations are:

$$\frac{\partial\zeta}{\partial t} - \frac{\partial\kappa}{\partial t} + \frac{1}{r}\frac{\partial}{\partial r}\left[r(\zeta + h - \kappa)v_r\right] + \frac{1}{r}\frac{\partial}{\partial\theta}\left[(\zeta + h - \kappa)v_\theta\right] = 0 \tag{1}$$

$$\frac{\partial v_r}{\partial t} - f v_\theta = -g\frac{\partial\zeta}{\partial r} - \frac{F_r}{\rho\,(\zeta + h - \kappa)} \tag{2}$$

$$\frac{\partial v_\theta}{\partial t} + f v_r = -\frac{g}{r}\frac{\partial\zeta}{\partial\theta} - \frac{F_\theta}{\rho\,(\zeta + h - \kappa)} \tag{3}$$

where
v_r = radial component of velocity of the sea water
v_θ = tangential component of velocity of the sea water
F_r = radial component of frictional resistance at the sea bed
F_θ = tangential component of frictional resistance at the sea bed
f = Coriolis parameter = $2\,\Omega\,\sin\varphi$
Ω = angular speed of the earth
φ = latitude of the location
g = acceleration due to gravity
κ = sea floor deformation

The parameterizations of F_r and F_θ are done by conventional quadratic law:

$$F_r = \rho\; C_f v_r \sqrt{{v_r}^2 + {v_\theta}^2} \quad \text{and} \quad F_\theta = \rho\; C_f v_\theta \sqrt{{v_r}^2 + {v_\theta}^2} \tag{4}$$

where ρ is the sea water density and C_f is the friction coefficient.

2.2. *Boundary Conditions*

For a closed boundary the normal component of velocity is considered as zero. Radiation type of boundary conditions are used for open boundaries which allow the disturbance created within the analysis area to go out of the area. The model area is bounded by the straight lines $\theta = 0$ and $\theta = \Theta$

through the pole O and the circular arc $r = R$ with center at O. Following Roy et al. (1999) northern, southern and western open sea boundary conditions are respectively

$$v_\theta + \sqrt{(g/h)}\,\zeta = 0 \quad \text{along } \theta = 0 \tag{5}$$

$$v_\theta - \sqrt{(g/h)}\,\zeta = 0 \quad \text{along } \theta = \Theta \tag{6}$$

$$v_r - \sqrt{(g/h)}\,\zeta = 0 \quad \text{along } r = R \tag{7}$$

2.3. ***Transformation in the radial direction***

For uniform grid of size $\Delta\theta$ in the tangential direction, the arc distance between two consecutive radial grid lines decreases towards the pole and increases away from the pole. Thus the arc distance increases as we move away from the coast although the grid size $\Delta\theta$ is constant. To obtain uneven resolution in the radial direction (fine to coarse), according to Haque et al. (2003), the following transformation is used:

$$\eta = c \ln\left(1 + \frac{r}{r_0}\right) \tag{8}$$

where, r_0 is of the order of total radial distance of the analysis area and c is a scale factor. From this transformation we obtain a relationship between Δr and $\Delta\eta$ which is as follows:

$$\Delta r = \frac{r + r_0}{c} \Delta\eta \tag{9}$$

This relation shows that keeping a constant value of $\Delta\eta$, we can generate variable Δr, which increases with increase of r. So, we obtain uneven resolution (fine to coarser) in the radial direction in the physical domain while in the computational domain ($\eta\theta$ -plane) the resolution remains uniform. Using the above transformation, equations (1) – (3) transform to:

$$\frac{\partial\zeta}{\partial t} - \frac{\partial\kappa}{\partial t} + \frac{c e^{-\eta/c}}{r_0 (e^{\eta/c} - 1)} \frac{\partial}{\partial\eta} \left\{ (\zeta + h - \kappa)(e^{\eta/c} - 1) v_r \right\} + \frac{1}{r_0 (e^{\eta/c} - 1)} \frac{\partial}{\partial\theta} \left\{ (\zeta + h - \kappa) v_\theta \right\} = 0 \tag{10}$$

$$\frac{\partial v_r}{\partial t} - f v_\theta = -\frac{g c e^{-\eta/c}}{r_0} \frac{\partial\zeta}{\partial\eta} - \frac{C_f v_r \sqrt{v_r^2 + v_\theta^2}}{(\zeta + h - \kappa)} \tag{11}$$

$$\frac{\partial v_\theta}{\partial t} + f v_r = -\frac{g}{r_0 (e^{\eta/c} - 1)} \frac{\partial\zeta}{\partial\theta} - \frac{C_f v_\theta \sqrt{v_r^2 + v_\theta^2}}{(\zeta + h - \kappa)} \tag{12}$$

The boundary conditions (5)-(7) remain unchanged due to this transformation.

3. GRID GENERATION AND NUMERICAL SCHEME

Pole of the coordinate system is located in the mainland of Penang at O ($5^{o}\,22.5'$N, $100^{o}\,30'$ E) and the model area extends from Penang in Peninsular Malaysia to the west of Sumatra (Fig.1).

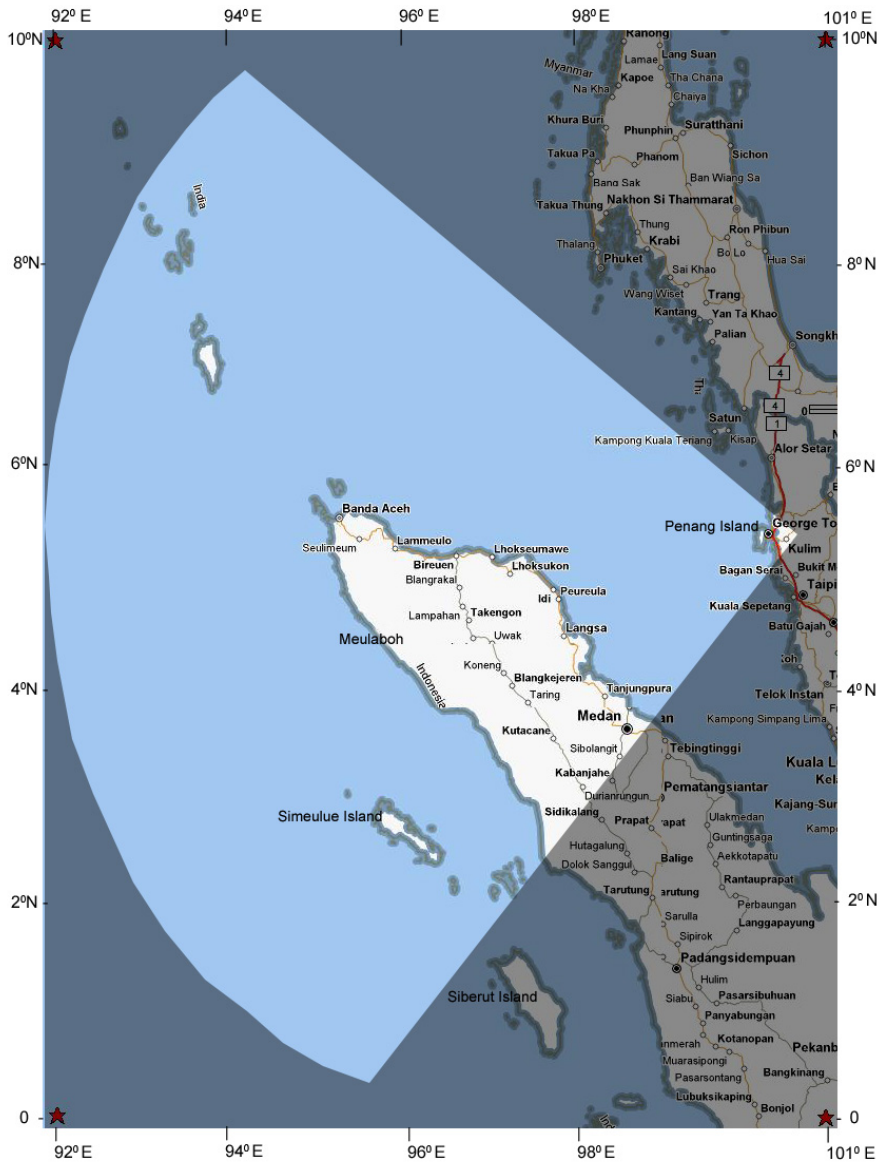

Figure 1: Map of the model domain including North Sumatra and Penang Island

The orthogonal grid system is generated through the intersection of a set of straight lines through O given by θ = *constant* and a set of concentric circles, with centre as O, given by r =

constant. The angle between any two consecutive radial lines is $\Delta\theta = 0.3333^0$, whereas the distance between two successive circular grid lines, Δr, increases as we proceed towards the open sea. After the transformation (8), both $\Delta\theta$ and $\Delta\eta$ become uniform. In the transformed domain the discrete grid points (η_i, θ_j) are defined by:

$\eta_i = (i-1)\,\Delta\eta; \quad i = 1, 2, 3, \ldots, M$

$\theta_j = (j-1)\,\Delta\theta; \quad j = 1, 2, 3, \ldots, N$

where, $M = 778$ and $N = 277$ also $\Delta\theta = 0.3333^o$ and $\Delta\eta = 1/1077$, so that in the computational domain η ranges from 0 to 777/1077. Although $\Delta\eta$ is taken as a constant, Δr increases with r according to the Eq. (9) and varies from 0.5 km to 1.0 km. Thus we obtain a finer mesh near the coast and gradually coarser mesh in the deep sea.

The sequence of time is given by:

$$t_k = k\Delta t; \qquad k = 1, 2, 3, \ldots \tag{13}$$

Although, in the physical domain N grid lines meet at the Pole, in the computational domain this point is considered as N distinct grid points which are generated automatically. Since the pole is considered at the land, where no computation is done, there is no problem of instability during numerical computation. In the computational domain a staggered grid system is used, which is similar to Arakwa C system.

The governing equations (10) – (12) and the boundary conditions (5) – (7) are discretised by finite-differences (forward in time and central in space) and are solved by a conditionally stable semi-implicit method. Moreover, the CFL criterion has been followed in order to ensure the stability of the numerical scheme. Along the closed boundary, the normal component of the velocity is considered as zero, and this is easily achieved through appropriate stair step representation as mentioned earlier. The time step is taken as 5 seconds that ensures stability of the numerical scheme. In the solution process, the value of the friction coefficient C_f is taken as 0.0033 throughout the physical domain. The depth data used in this study are collected from the Admiralty bathymetric charts.

4. INITIAL CONDITION

The generation mechanism of the 26 December Indonesian tsunami is mainly due to the static sea floor uplift caused by abrupt slip at the India/Burma plate interface. A detailed description of the estimation, based on Okada (1985), of the extent of earthquake rapture (92°E to 97°E and 3°N to 10°N) along with the maximum uplift (507 cm) and subsidence (474 cm) of the seabed has been reported in Kowalik et al. (2005). According to this estimation, the source is elongated along the fault zone from south-east to north-west with uplift to subsidence from west to east. Following Kowalik et al. (2005), a source, of the same extent with maximum rise of 5 m and maximum fall of 4.75 m of the sea surface, is assigned as the initial condition. The vertical cross section of the source along 121st grid line is shown in Fig. 2. Other than source region, the initial sea surface elevations are taken as zero everywhere. Also the initial radial and tangential components of velocity are taken as zero throughout the domain.

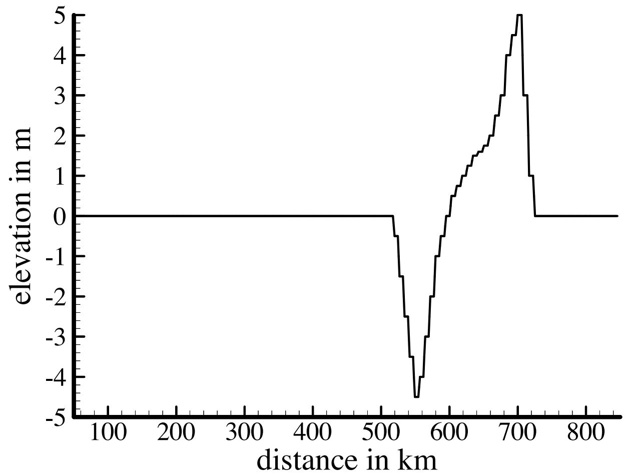

Figure 2: Vertical cross-section of the source along 121st grid line

5. RESULTS AND DISCUSSIONS

The effects of the Indonesian tsunami of December 2004 along the coasts of North Sumatra and Penang Islands are investigated. Numerical simulation of this potential tsunami is performed in the framework of linear shallow-water equations in cylindrical polar coordinate system.

5.1. Simulated water levels along North Sumatra

Figure 3 describes the computed time series of water levels at two locations of North Sumatra along east and west coasts. The maximum elevation of the water level near the coastline of Banda Aceh (north-west of Sumatra) is approximately 9.2 m (Fig. 6a). At approximately 20 min after the generation, the water level starts decreasing and reaches the level of -4.4 m. Then the water level increases continuously to reach a level of 9.2 m before going down again and the oscillation continues for several hours. The computed result also shows the withdrawal of water from the coastal region before arrival of high surge. The computed time series of water level at Medan coast (north-east of Sumatra) indicates that the maximum elevation along this coast is 3 m and that the arrival of tsunami surge is preceded by the withdrawal of water (Fig.3b). The oscillations continue for several hours in both the locations and the damping is rather slow.

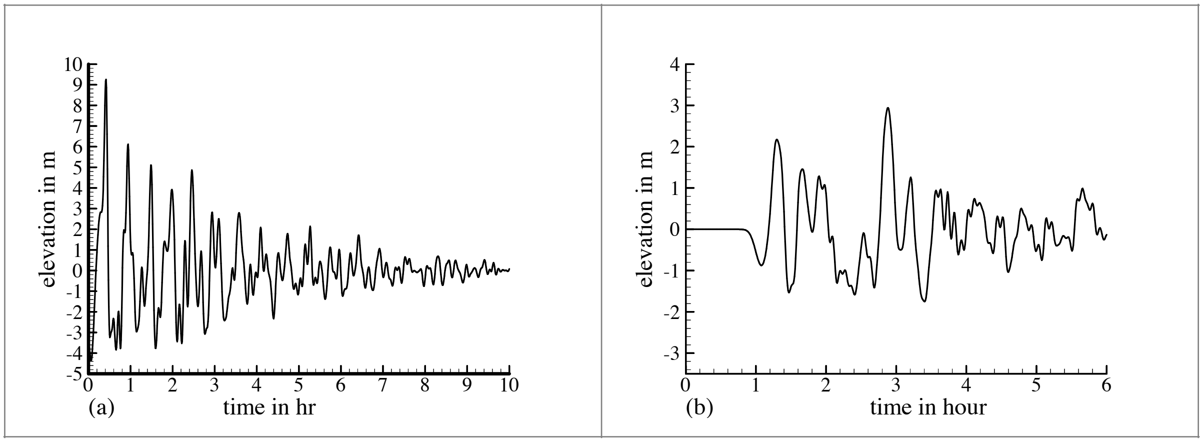

Figure 3: Time series of computed elevation at coastal locations of Sumatra Island associated with the tsunami source at Sumatra 26 December, 2004: (a) Banda Aceh, (b) Medan coast The computed results indicate that the North Sumatra is vulnerable for very strong tsunami surges due to the permanent source near Sumatra along the Burma/India interface.

This can be seen from Fig. 4, where the curves of maximum elevations have been drawn along the west and east coasts of North Sumatra. The maximum elevation along the east coast has exceeded 15 m at Medan (Fig. 4a).

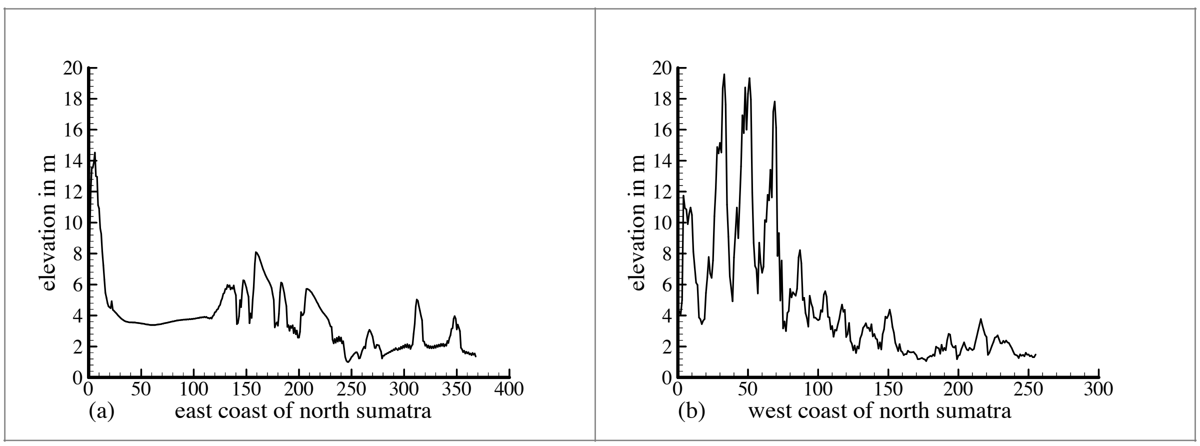

Figure 4: Maximum elevation associated with source 26 December 2004 at Sumatra along the north coasts of Sumatra Island: (a) east coast, (b) west coast On the other hand, the surge intensity is found to be highest at the west coast; the highest elevation in excess of 17 m is attained at the north of Meulaboh (Fig. 4b).

The same intensity of surge is attained along the Simeulue Island, which is located at the west of North Sumatra. The computed peak elevation surrounding the North Sumatra can be seen from the contour plot of maximum elevation in Fig. 5. From the contour plot it is evident that that the surge amplitude is increasing very fast near the north-west part of Sumatra.

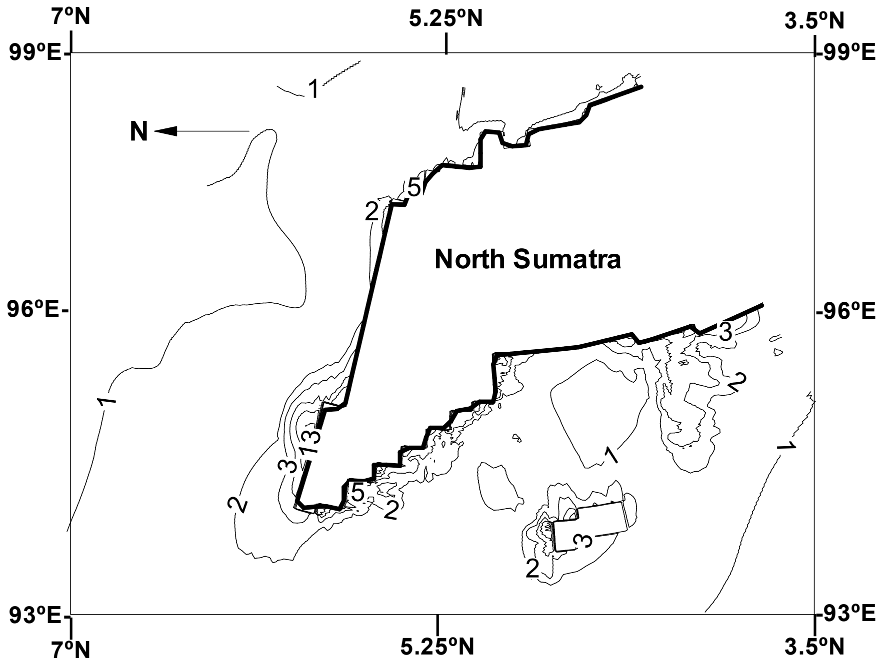

Figure 5: Contour of maximum water levels around the two coasts of North Sumatra.

Table 1. Observed and computed water levels above the mean sea level at different locations of Penang Island. (Source: The authors conducted this survey)

Location name	Observed water level (m)	Computed water level (m)
Batu Ferringhi (north penang)	3.3	3.2
Taluk Bahang	> 2.0	2.62
Tanjung Tokong	2.80	1.0
Tanjong Bunga	3.0	2.5
Pasir Panjang	>2.0	3.2
Kuala Pulau Betung	2.0	2.24

5.2. Simulated water levels along Penang Island

The water levels at different locations of the coastal belt of Penang Island are also stored at an interval of 30 seconds. Fig. 6 depicts the computed time series of water levels at two locations on the north and west coasts of Penang Island. The maximum amplitude at Batu Ferringhi (north coast) is approximately 2.6 m (Fig. 6a).

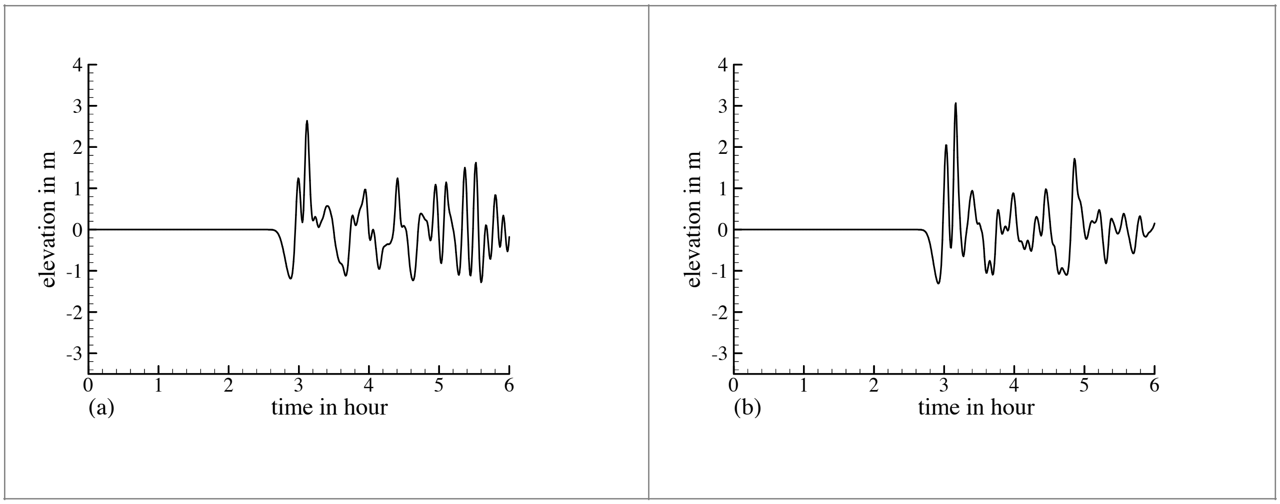

Figure 6: Time series of computed elevation at two coastal locations (a) Batu Ferringhi, (b) Pasir Panjang of Penang Island associated with the tsunami source at Sumatra 26 December, 2004.

It is seen that at approximately 2.80 hrs after the generation of tsunami at the source, the water level starts decreasing (withdrawal of water) and reaches level of -1.2 m. Then the water level increases continuously to reach a level of 2.7 m at 2 hrs 40 min before going down again. The computed water level at Pasir Panjang (west coast) shows the same pattern as that of Batu Ferringhi with the maximum water level of approximately 3.2 m (Fig. 6b). The computed results indicate that the west coast of Penang Island is vulnerable for very strong tsunami surges due to the permanent source near Sumatra.

This can be seen from Fig. 7, where the curves of maximum elevations have been drawn along two coastal belts of Penang Island. The maximum elevation along the west coast (north to south) has exceeded 3.6 m at Tanjong Bunga (Fig. 7a). On the other hand, the surge intensity is found to be highest at the north coast; the highest elevation in excess of 2.7 m is attained at Teluk Bahang (Fig. 7b).

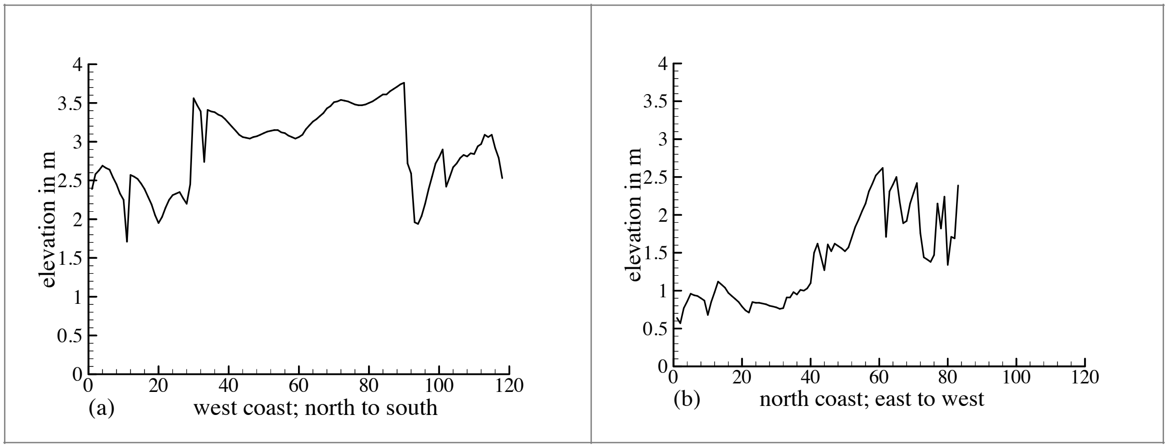

Figure 7: Maximum elevation associated with source 26 December 2004 at Sumatra along two coasts of Penang Island: (a) west coast, (b) north coast

The computed peak elevation surrounding the Penang Island is also presented in the contour plot (Fig. 8). From the figure it is clear that the surge amplitude is increasing very fast near the shore of the Penang Island. The computed results show that the west coast of Penang Island is vulnerable to a stronger tsunami surge.

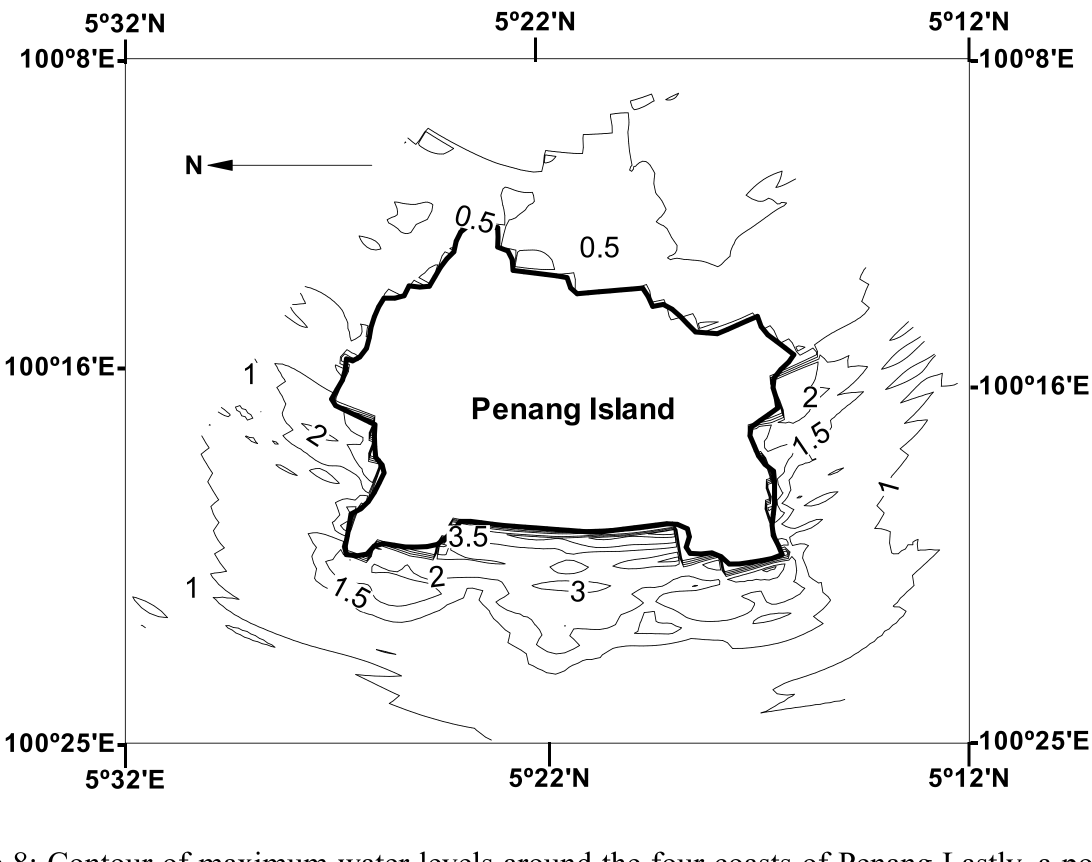

Figure 8: Contour of maximum water levels around the four coasts of Penang Lastly, a post tsunami survey report on water levels at different locations of Penang Island, along with the computed water

levels, is shown in Table 2. It is found that agreement between the simulated and observed values is satisfactory.

Table 2. Observed and computed water levels above the mean sea level at different locations of North Sumatra

Location name	Observed maximum tsunami amplitude near the shore	Computed water level
Simeulue Island	> 3 m	3.4 m
Meulaboh	1.5 m	1.8 m
Medan	>2.5 m	2.9 m
Banda Aceh	-	9.2 m
Meulaboh Aronghan	15 m	> 14 m
St 176, WPT 17	> 15 m	18 m

Source: measured by the Turkish-Indonesian-USA team during the field survey on Sumatra on January 21-29, 2005

6. CONCLUSIONS

In this paper, the model of Ismail et al. (2006) has been used to simulate the water levels along North Sumatra and Penang Island in Peninsular Malaysia. The simulated results are found to be in good agreement with the observed data collected through post tsunami surveys. The computed results indicate that the linear polar coordinate shallow water model is able to estimate the effects of tsunami along Sumatra and Penang islands in Peninsular Malaysia with realistic accuracy.

REFERENCES

Haque, M.N.; Miah, S., Roy, G.D.;(2003): A Cylindrical Polar Coordinate Model with Radial Stretching for the coast of Bangladesh, Proc. Int. Conf. App. Math. & Math. Phy. (ICAMMP), Shahjalal Univ. of Sc. & Tech. Sylhet, Bangladesh, pp 77-87.

Ismail, A. I. M., Karim, M. F., Roy, G. D. (2006): “Simulation of Tsunami along Sumatra and Penang Islands Associated with the Indonesian Tsunami of 26 December 2004 using a Linear Polar Coordinate Shallow Water Model”. International Conference. on Mathematical Modelling and Computation, University Brunei Darussalam, Brunei. 5 - 8 June 2006.

Imamura. F.; Gic,E.C.;(1996): Numerical Model for Tsunami Generation due to Subaqueous Landslide Along a coast- A case study of the 1992 Flores tsunami, Indonesia; Sc. Tsunami Hazards, 14 (1): 13-28.

Imteaz. A. M.; Imamura. F.;(2001): A Non-Linear Numerical Model for Stratified Tsunami Waves and its Application, Sc. of Tsunami Hazards, Vol.19, pp.150-159.

Iguchi, T. (2011): “A mathematical analysis of tsunami generation in shallow water due to sea bed deformation,” Proceedings of the Royal Society of Edinburgh, 141A, 551-608.

Karim, M. F.; Sankar, D. S.; Yunus, E. (2016): “On the open sea propagation of 2004 global tsunami generated by the sea bed deformation, “International Journal of Applied Engineering Research, 11 (4) 2686-2692.

Karim, M. F., Roy, G. D., Ismail, A. M., Meah, M. A. (2007): “A shallow water model for computing Tsunami along the west coast of Peninsular Malaysia and Thailand using boundary-fitted curvilinear grids,” Journal of Science of Tsunami Hazards, Volume 26, No. 1, 21 - 41.

Kowalik. Z.; Knight. W.; Logan. T.; (2005) Whitmore. P.:Numerical Modeling of The Global Tsunami, Sc. of Tsunami Hazards, Vol.2, No.1, pp.40.

Okeda, Y. (1985): Surface Deformation due to Shear and Tensile Faults in a Half Space; Bull. Seism. Soc. Am., 75: 1135-1154.

Roy, G. D., Karim, M. F., Ismail, A. I. M. (2007): A Non-Linear Polar Coordinate Shallow Water Model for Tsunami Computation along North Sumatra and Penang Island. Journal of Continental Shelf Research, 27, 245–257.

Roy, G. D., (1995): Estimation of expected maximum possible water level along the Meghna estuary using a tide and surge interaction model. Environment International. 21(5), 671-677.

Roy, G.D.; Humayun Kabir, A.B.;Mandal, M.M.; Haque, M.Z.(1999): Polar Coordinate Shallow Water storm surge model for the coast of Bangladesh, Dyn. Atms. Ocean, 29, 397-413.

Roy, G. D., Izani, A. M. I. (2005): An investigation on the propagation of 26 December 2004 tsunami waves towards the west coast of Malaysia and Thailand using a Cartesian coordinates shallow water model, Proceedings of the International Conference in Mathematics and Applications, Mahidol University, Thailand, 389-410.

Titov,V.V., Gonzalez, F.I. (1997): Implementation and Testing of the Method of Spliting Tsunami (MOST) Model; NOAA Technical Memorandum ERL, PMEL -112, Contribution No. 1927 from NOAA/Pacific Marine Environmental Laboratory: pp 11.

Yalciner, A. C., Karakus, H., Ozer, C and Ozyurt, G. (2005): Understanding the generation, propagation, near and far field impacts of tsunamis, Lectures Notes, Middle East Tech. Univ., Ankara, Turkey